

## Multiproxy evidence of Mid-Pleistocene dry climates observed in calcretes in Central Turkey

Ceren KÜÇÜKUYSAL<sup>1\*</sup>, Asuman GÜNAL TÜRKMENOĞLU<sup>2</sup>, Selim KAPUR<sup>3</sup>

<sup>1</sup>Geological Research Department, General Directorate of MTA, Building G, Room 204, 06800 Çankaya, Ankara, Turkey

<sup>2</sup>Department of Geological Engineering, Middle East Technical University, 06800 Ankara, Turkey

<sup>3</sup>Department of Soil Science, Çukurova University, 01330 Balcalı, Adana, Turkey

Received: 21.02.2012 • Accepted: 19.09.2012 • Published Online: 06.05.2013 • Printed: 06.06.2013

**Abstract:** Palaeosols are very important in reconstructing palaeoclimate studies, since they are accepted as useful climate markers and as potential providers of proxy data. The study of the palaeosols of the Plio-Pleistocene rock sequences around Ankara revealed evidence for a reconstruction of the Quaternary palaeoclimate of the region. The study area is located in Bala, south-east of Ankara, which contains Middle Pleistocene red palaeosols with powdery to nodular calcrete developments, alternating with channel deposits. During this warm and arid period in the Pleistocene, the limited water available in the soil led to the accumulation of low magnesian carbonates, forming calcretes. The clay fractions of the samples were X-rayed using air-drying, ethylene-glycol solvation and heating treatments. The clay mineral contents were determined as smectite, kaolinite, illite and chlorite. Palygorskite was also identified. In the relative abundances of clay minerals, smectite, the most abundant clay mineral, is depleted towards the upper part of the section while the amount of palygorskite increases. Since palygorskite is the only pedogenic mineral formed during the Pleistocene, its presence can be accepted as evidence of the dominant arid climatic conditions. The isotopic composition of carbonates in the Bala section exhibits a slightly wider range in  $\delta^{13}\text{C}$  composition from  $-5.98\text{‰}$  to  $-9.22\text{‰}$  and a narrower range in  $\delta^{18}\text{O}$  composition from  $-7.19\text{‰}$  to  $-8.66\text{‰}$ . The carbon isotope values clearly imply that arid to semiarid flora C4 is dominant, with C3:C4 mixed vegetation. This study suggests that the Middle Pleistocene is the time of the Mid-Brunhes Event when the dominantly warm climatic temperatures led to the development of calcretes in Bala, Ankara, as with all Quaternary Mediterranean-type calcretes.

**Key Words:** Pedogenic, clay minerals, palaeosol, palygorskite, calcrete, arid climate, Ankara, Quaternary

### 1. Introduction

During the Late Cenozoic, there were 2 relatively abrupt climate transitions. These are the onset of major northern hemisphere glaciation approximately 2.7 Myr ago and the mid-Pleistocene transition (MPT) or mid-Pleistocene revolution (MPR) (Pisias & Moore 1981; Ruddiman *et al.* 1989; Imbrie *et al.* 1993; Candy *et al.* 2010) when the dominant periodicity of glacial response changed from 41 to 100 kyr (Lisiecki & Raymo 2007). The MPT had a great effect on the temperature and precipitation patterns over the European continent, from interglacial to glacial periods (Ermolli & Cheddadi 1997). Following the periodicity changes, starting from the Middle Pleistocene (780–450 ka) to the Holocene, a warming period called the Mid-Brunhes Event (MBE) occurred (Candy *et al.* 2010). Currently, the MBE has not been proved either as a global phenomenon or as being effective only in specific regions. However, Quaternary calcretes are good proxies to define the impact of the MBE across the Mediterranean. Calcretes are defined as the near-surface carbonate accumulations in

continental environments. They are considered as possible products of a warm mid-Pleistocene period (Kapur *et al.* 1987, 2000).

Recently, numerous studies relating to the Quaternary palaeoclimate of Turkey were conducted, especially concerning pollen assemblages in lakes, as well as sediment contents in caves as potential proxy sources (Bottema *et al.* 1993, 1994; Eastwood *et al.* 1999; Fontugne *et al.* 1999; Kuzucuoğlu *et al.* 1999; Wick *et al.* 2003; Litt *et al.* 2009; Göktürk *et al.* 2011; Roberts *et al.* 2011). Among the major climate-dependent parameters, palaeosols make an important contribution for such scientific evaluations (Bradley 1999). Although palaeosols have been recognised widely in Turkey and studied in terms of their soil properties (Cangir & Kapur 1984; Kapur *et al.* 2000), most have not been directly evaluated for the Quaternary palaeoclimates.

The purpose of this study was to employ the clay proxy data and the geochemical characteristics of the palaeosols and carbonates in a calcrete section to reconstruct

\* Correspondence: [kucukuysal09@yahoo.com.tr](mailto:kucukuysal09@yahoo.com.tr)

Quaternary palaeoclimates in Ankara (Central Anatolia, Turkey). An additional attempt was made to test whether the MBE affected the study area in forming calcretes.

## 2. Geological setting and description of the calcrete section

The study area is located in Ankara, to the southeast of Bala, near Çavuşlu village (Figure 1A). The most recent studies in the region (Akyürek *et al.* 1997; Akçay *et al.* 2008; Dönmez *et al.* 2008) have defined the geology of the study area. This section summarises both the studies mentioned above and the field findings. The Late Cretaceous Artova ophiolitic melange is the oldest unit in the study area (Figure 1B). It contains serpentinite, radiolarite, gabbro, diabase, spilitic basalt and limestone blocks of Triassic age. It is overlain unconformably by the Middle Eocene Baraklı formation. It is formed by alluvial fan deposits of red conglomerate, sandstone and mudstones (Figure 1B). The Baraklı Formation has a lateral and vertical transition into the overlying Çayraz formation, which is a transgressive unit containing sandstones, claystones and limestones of Middle Eocene age. The Çavuşlu volcanics are composed of spilitic basalts, basic lavas and pyroclastics shown by their stratigraphic position to be of Early-Middle Eocene age. They are overlain unconformably by the Late Eocene-Oligocene İncik formation, formed of regressive-type evaporites, cross- and parallel-laminated continental conglomerates and sandstones. Among the younger units in the region, the Middle-Late Eocene Kumartaş formation, composed of fluvial and lacustrine sediments, unconformably overlies all the older units in the region. Above is the Hançılı formation, composed of conglomerate, sandstone, siltstone, marl, clayey limestone and tuff alternations and, locally, gypsum with shale. It is unconformably overlain by the Middle Miocene-Pliocene undifferentiated continental sedimentary rocks of the Central Anatolian group, which interfingers with basaltic, evaporitic and lacustrine rocks. The youngest unit in the study area is Quaternary alluvium (Figure 1B).

The studied section is in undifferentiated continental rocks (Central Anatolian Group) consisting of red alluvial deposits alternating with channel deposits (Figure 2). The presence of soil features (soil horizons with structure and biological activity) in the reddish brown mudrocks can be attributed to the presence of palaeosols with overlying calcretes. Küçükuysal (2011) stated that the presence of pedofeatures, such as clay cutans, floating grains, circumgranular cracks, MnO linings, secondary carbonate rims, indicators of past bioturbation and remnants of root fragments, all document that the studied reddish alluvial deposits are palaeosols and the carbonate concretions represent the calcretes. The palaeosol layers have sharp upper contacts with the overlying channel deposits (Figure

2). The calcretes are nodular, tubular and powdery in form and show downward transitional gradations (Figure 2).

A 40.5-m section was studied, using continuous core drill samples and collected field samples along a measured section, for its clay mineralogy and isotope geochemistry (Figure 3). At the bottom of the sampled section, channel deposits were found, composed of well-sorted gravels with subangular to subrounded grains. Basalt and andesitic basalt fragments are common at these levels. At the bottom layer, the mudstones are browner and have Munsell colours of 7.5YR 6/6. Up section, the brown mudstone layers intergrade with blocky to subangular blocky ped structures with a Munsell colour of 2.5YR 4/4 and 5YR 7/2 (Figure 3). These were all developed in the Late Pleistocene, since the Middle Pleistocene was the period of formation of C1 and C2 calcrete layers dated by the electron spin resonance (ESR) technique (Küçükuysal *et al.* 2011). Soil structural peds were subangular blocky to prismatic in structure, implying the occurrence of drier conditions. The colour of the mudstones (palaeosols) becomes more reddish and the frequency of the calcrete layers increases towards the upper part of the section (Figure 3).

## 3. Materials and Methods

Palaeosol carbonates, generally calcretes, are of the utmost significance in interpreting semiarid to arid climatic conditions (James 1972; Goudie 1973, 1983; Tucker 1991). Calcrete is defined as a terrestrial product within the zone of weathering, in which calcium carbonate ( $\text{CaCO}_3$ ) has accumulated and/or has replaced a preexisting soil, rock, sediment or weathered material to give a substance that may ultimately develop into an indurated mass (Goudie 1973; Salomons *et al.* 1978; Wright & Tucker 1991; Eren 2011). Our study is based on the definition given by Wright and Tucker (1991), which stated that the calcrete is a near-surface, terrestrial accumulation of predominantly calcium carbonate, which occurs in a variety of forms from powdery to nodular to highly indurated, resulting from the cementation and displacive/replacive introduction of calcium carbonate into soil profiles, bedrock and sediments in areas where vadose and shallow phreatic groundwaters become saturated in calcium carbonate.

The mineralogical and chemical composition of pedogenic phyllosilicates, i.e. the proxies of palaeoclimatic reconstruction, form in a soil through the alteration of detrital clays and by primary precipitation, and are strongly controlled by the chemical activity of the soil solution, which in turn is influenced by the amount and seasonality of rainfall (Buol *et al.* 1997; Tabor 2002). Two calcrete samples, 7 m apart from each other, in the Bala section have ESR ages of  $761 \pm 120$  ka (C1, the bottom unit) and  $419 \pm 64$  ka (C2, the upper unit) (Küçükuysal *et al.* 2011). This means that the ages of the calcretes

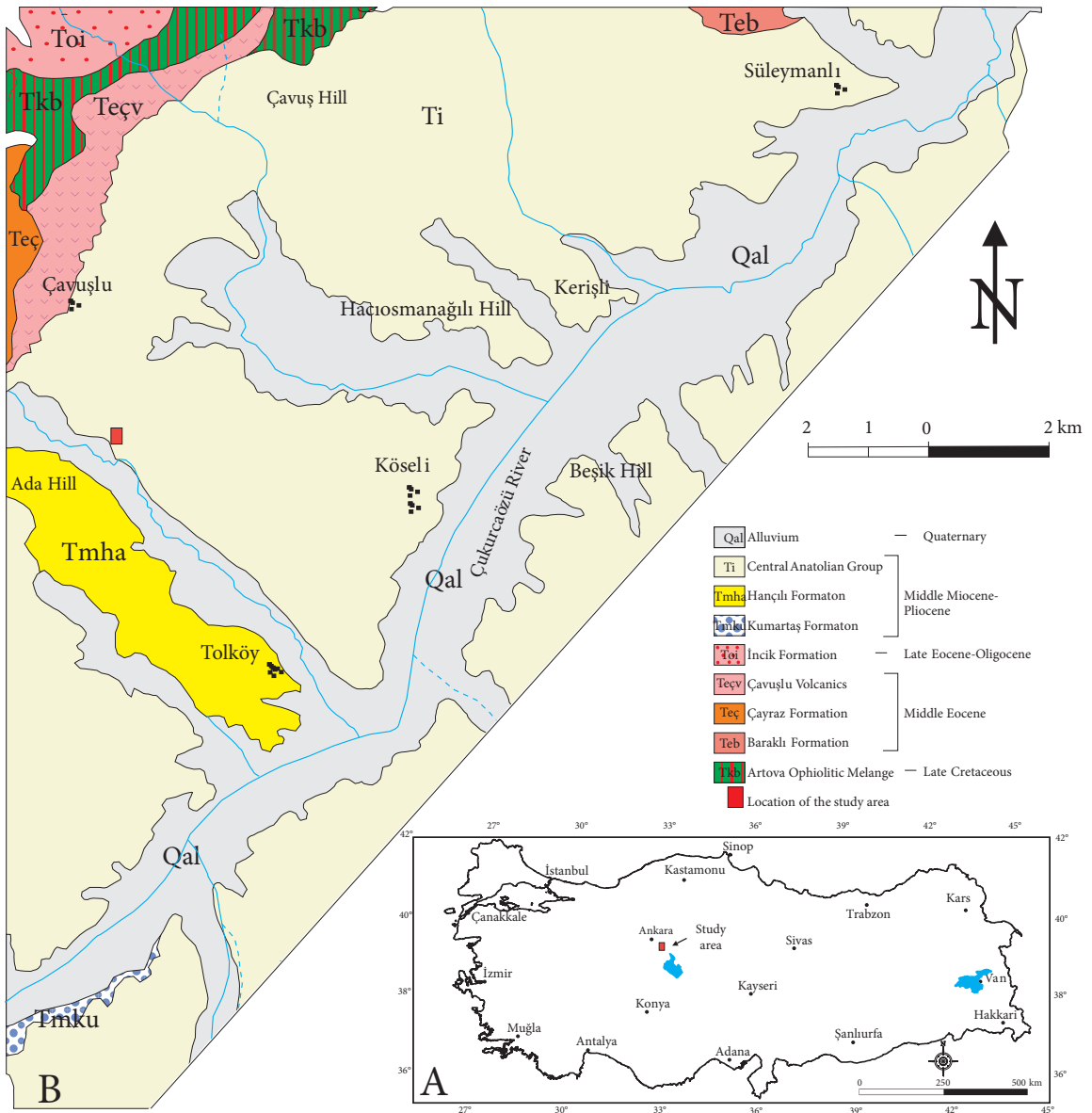


**Figure 1.** A) Map of Turkey showing the location of Ankara and Bala; B) Geological map of the study area showing the positions and the ages of the lithological units and the location of the Bala section (from Dönmez *et al.* 2008).

are Middle Pleistocene, which is consistent with their stratigraphic positions.

During this study, the combined methods of Thorez (1976), Jackson (1979), Brindley (1980) and Moore and Reynolds (1989) were applied to separate the clay fraction from the bulk palaeosols and to prepare them for X-ray powder diffraction analysis on glycol-solvated randomly oriented clay fractions. Eighteen levels were sampled from the Bala succession and 10 of them were X-rayed to define their bulk mineral compositions and the clay fractions. From top to bottom, samples are numbered from B-1 to B-17 and Bc, respectively. The relative abundances of

clay minerals were determined by the method of Biscaye (1965). Clay samples were scanned from  $2^\circ$  to  $30^\circ 2\theta$  in order to determine the first-order clay mineral peaks. The mineral abundances in the bulk fraction (size fraction of less than  $63 \mu\text{m}$ ) were determined according to the method of Gündoğdu (1982). Samples were selected for scanning electron microscopic (SEM) investigation with the QUANTA 400F field emission scanning electron microscope with 1.2 nm resolution. An energy dispersive X-ray spectrometer (EDX) was also employed on selected samples to obtain the element contents of the specific locations. Additionally, stable isotope compositions of

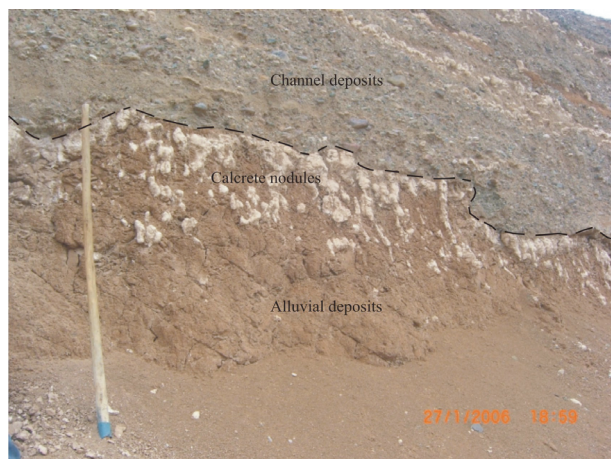


**Figure 2.** A picture of the studied section in which red alluvial deposits are seen together with calcrete formations alternating

with channel conglomerates (shovel length is 110 cm). The carbonate-bearing palaeosols were determined at the Laboratory for Stable Isotope Science in the Department of Earth Sciences at the University of Western Ontario, Canada. A multiprep device coupled to a VG Optima dual inlet stable isotope ratio mass spectrometer was used for this procedure.

#### 4. Implications of the results on a local scale

##### 4.1. Clay Mineralogy

Almost all of the samples have the same clay and nonclay minerals through the Bala succession. Nonclay minerals (quartz, feldspar and calcite) were identified within a size fraction of less than 63  $\mu\text{m}$  (Table 1). Quartz was determined by the presence of 2 prominent peaks at 4.27  $\text{\AA}$  and 3.34  $\text{\AA}$ . Feldspars, however, were determined by the most intense peak at 3.2  $\text{\AA}$ . Calcite was determined with a sharp and intense peak at 3.03  $\text{\AA}$  (Figure 4A).

The major clay minerals were smectite, kaolinite, illite and chlorite, with lesser amounts of palygorskite (Figure 4B). Smectite, the dominant clay mineral found in the Bala section, was identified by the shift from 14.6  $\text{\AA}$  to 17.7  $\text{\AA}$  on ethylene glycol solvation. Smectite collapses to 10.1–10.2  $\text{\AA}$  after heat treatment at 550  $^{\circ}\text{C}$  (Figure 4B). The ratio of  $v$  to  $p$  was determined to be less than 0.4, implying poor crystallinity of the smectite (Biscaye 1965) (Figure 4B). Illite, kaolinite and chlorite were all present in small quantities in the samples. Illite was detected by the 10.1  $\text{\AA}$  peak, but is recognised with difficulty on the diagrams because of its weak reflections. It is not affected by ethylene glycol solvation and heat treatments (Figure 4B). It also overlaps with smectite and partly with palygorskite when the basal reflections of these 2 minerals collapse to 10.1  $\text{\AA}$  on heating (Figure 4B). Kaolinite was identified with its basal reflection at 7.13  $\text{\AA}$ , which disappeared

after heating at 550  $^{\circ}\text{C}$ . The relatively small amount of chlorite in the samples was somewhat difficult to identify. The crystallinity of chlorite was moderate, with basal reflections at  $d(001)$  14  $\text{\AA}$ ,  $d(002)$  7.30  $\text{\AA}$  and  $d(003)$  4.7  $\text{\AA}$  (Figure 4B). Palygorskite was determined by its peaks at 10.4  $\text{\AA}$  and 6.4  $\text{\AA}$  (Figure 4B). Palygorskite was not affected by glycerol solvation, but its 10.4  $\text{\AA}$  peak collapsed to 10  $\text{\AA}$  on heating to 550  $^{\circ}\text{C}$  (Figure 4B). Palygorskite is present in almost all samples except B–10 and B–14, where it may also be present in small amounts and weakly crystalline.

Consistent amounts of quartz were present throughout the section, with a slight increase at the top. Its abundance varies in a narrow range between 4.7% and 8.6%. Feldspar shows a slight increase in the upper part of the sequence. Its abundance varies from 8.9% to 24.1%. Calcite, on the other hand, starts with a consistent amount at the bottom, then shows an increase in the middle of the section. Towards the top, calcite increases, as expected, and varies from 4.5% to 16.7%.

The clay mineral abundance usually exceeds 60% throughout the section (Table 2). Smectite, the most abundant clay mineral, shows both enrichment and depletion through the section, varying from 21.4% to 95.2%. It is relatively more abundant at the bottom of the section and becomes scarcer towards the top. Chlorite (3.6% to 16.7%), kaolinite (3.6% to 21.2%) and illite (5.9% to 28.6%) are present throughout the section. The amount of palygorskite, however, increases towards the top of the section from 2.9% to 14.3%.

Smectite is the dominant clay mineral in the clay fraction. It shows an alternation of enrichment and depletion patterns, with a general decreasing trend towards the top of the section. Palygorskite, on the other hand, increases towards the top of the section, indicating the presence of arid conditions in the past. The abundances of smectite and palygorskite show opposite variations in the palaeosols of the Bala section. This relationship may also indicate that smectite was a possible source of Mg for the formation of palygorskite. This is also confirmed by the SEM images of the Bala samples, showing calcite rhombohedra covered with palygorskite fibres, which also form bridge-like structures indicating in situ formation from the soil solution. Calcite shows a similar pattern to palygorskite, documenting the possibility of precipitation from the soil solution as a secondary mineral bearing a pedogenic history of the Bala section palaeosols.

##### 4.2. Scanning electron microscope investigations

Calcretes from the Bala section, as subaerial exposure surfaces, are mostly recognised within horizons very close to the surface and contain calcite (Figure 5A). Clay minerals form the matrix on which detrital grains float and pedogenic palygorskite forms a thin sheet. The formation of authigenic smectites was also observed with

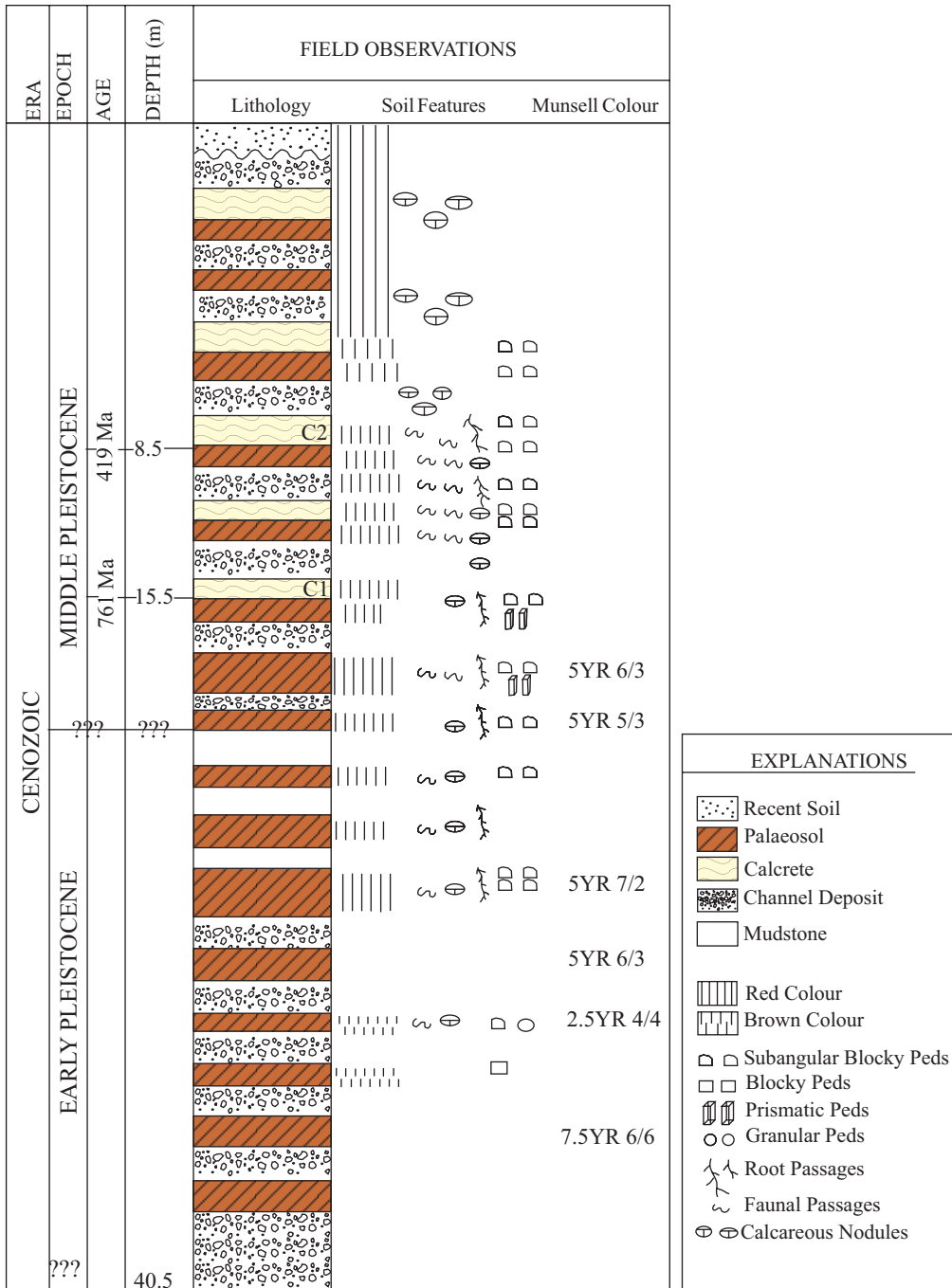


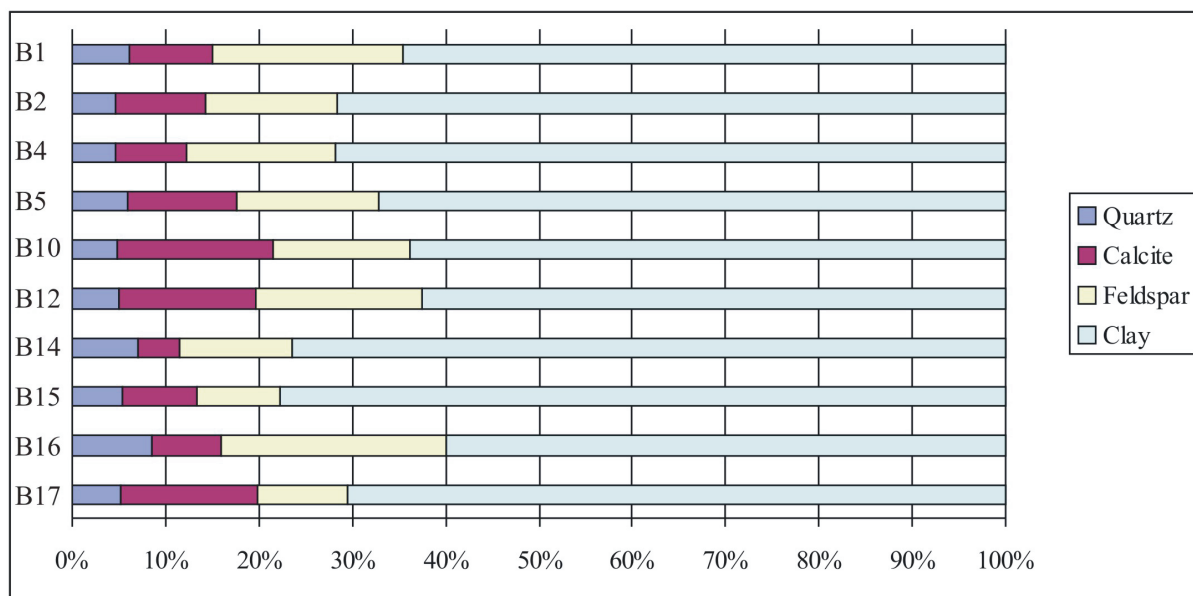
Figure 3. The Bala stratigraphic section with the descriptions of lithology, soil features and Munsell colours (C1 and C2 calcrite data from Küçükuyşal *et al.* 2011).

a nodular crystalline form (Figure 5B). Palygorskite fibres form bridge-like structures across calcite grains (Figure 5C). A different habit of chlorite recognised was a chlorite rosette in the Bala palaeosols (Figure 5D). Palygorskite fibres are randomly distributed over the clayey matrix and overlie the feldspar grains (Figure 5E). Quartz is euhedral to subhedral and cemented by a clayey matrix. Its fresh

surface is very clear and shows well-developed conchoidal fractures (Figure 5F).

4.3. Geochemistry

The mineralogical and chemical compositions of the palaeosols are strongly controlled by the geochemistry of the soil solution. Therefore, the geochemical characteristics of the palaeosols and their carbonates are clearly important

**Table 1.** Semiquantitative analysis of bulk composition of samples.

proxies revealing the climatic history of the soil. Like many studies on palaeosol geochemistry (Retallack 1997, 2001), more recently Sheldon and Tabor (2009) stated that different proxies based on geochemical analyses can be used to infer the pedogenic processes revealing the effect of chemical weathering in palaeosols (Table 3). The ratios revealing the degree of hydrolysis, oxidation, acidification, salinisation and leaching are all related to the pedogenic processes.

The molecular weathering ratios of the typical major oxides and carbonates of the palaeosols were calculated along with salinisation, which is the indicator for the past prevalently arid conditions, reflecting the relative leaching of sodium to potassium in surficial horizons. The salinity ratio ranges from 0.3 to 2.7 for the Bala palaeosols and calcretes (Figure 6), documenting an enrichment close to the upper limit as evidence of evaporation during palaeosol pedogenesis. However, salinity for arid climatic conditions should exceed 1, as in this study, which is 2, with positive enrichments in the B11, B12 and B14 carbonate-rich horizons (Figure 6). Calcification is very high at the top due to the presence of carbonate nodules, with enrichment at the B11 and B12 horizons. Calcification is positively correlated with salinity, indicating that the saline conditions favoured the accumulation of carbonates (Figure 6). Moderate clayeyness varies from 0.15 to 0.3. Leaching shows an increasing trend towards the top of the section, which is consistent with the other results. Leaching ranges from 1 to 3 in the Bala section, implying 2 major shifts greater than the leaching value of 2 in the B6

and B11 horizons, which can be accepted as the surficial horizons of the palaeosols (Figure 6).

The chemical index of alteration (CIA) of the Bala section has also been calculated using the formula of Nesbitt and Young (1982), using molecular proportions of some elements. The higher the value, the more intense the weathering has been. Maximum CIA values of calcretes are 15, whereas the palaeosol CIA levels generally exceed 50. The other measure for the chemical index of alteration, CIA-K, is also very similar to the CIA values: low for calcretes and high for palaeosols. The CIA and CIA-K versus depth diagrams plot parallel to each other. Both indices show that the section experienced moderate weathering conditions in the geological past (Figure 6).

Molecular weathering ratios of the palaeosols and the calcretes of the Bala section display a parallel trend between calcification and salinisation, which increase towards the upper section. This implies increasing aridity with increasing temperature (Figure 6). The chemical index of alteration values of CIA-K show major shifts at the B1 and B11 levels, with very high values indicating a high degree of chemical alteration (Figure 6). The values of CIA-K generally exceed 50, which indicates a medium degree of weathering. The lower values fall in the carbonate-rich levels of the Bala section (Figure 6). All of these values suggest the occurrence of a wet powdery calcrete formation environment. The wet conditions, on the other hand, progress via the pluvials and favour the formation of eluviation zones, where leaching values are high.

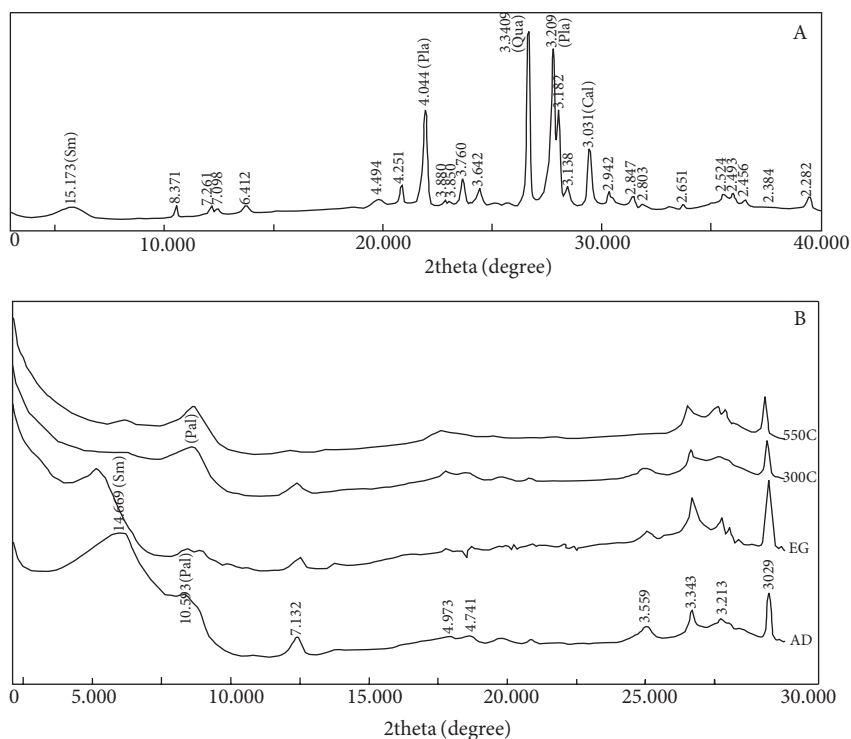


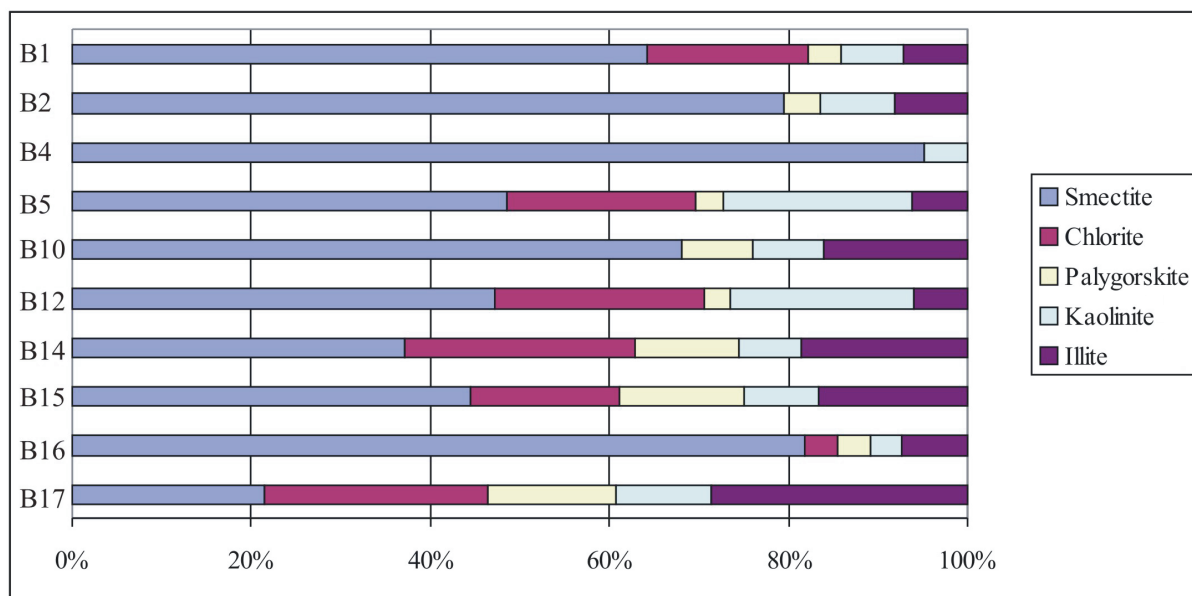
**Figure 4.** A) X-ray diffraction of powder representative B-2 sample from the Bala section (Sm: smectite; Pla: plagioclase; Qua: quartz; Cal: calcite); B) X-ray diffraction pattern of the sample with air-dried, ethylene-glycolated, and heat-treated samples of the Bala section (Sm: smectite; Chl: chlorite; Kao: kaolinite; Qua: quartz; Cal: calcite; Pal: palygorskite; AD: air-dried; EG: ethylene-glycolated; 300 °C and 550 °C: heating treatments).

#### 4.4. Stable isotope geochemistry

Stable isotope data are widely preferred in palaeoclimatology studies, since they are accepted as good proxies reflecting changes in environmental conditions. The stable isotopic ratios of carbon and oxygen from authigenic soil carbonate can record changes in climatic conditions and plant cover. Using these ratios from carbonate nodules that formed in stacked palaeosols within ancient fluvial deposits can provide a proxy for changing climatic conditions (White 2005). The carbon isotopic composition of authigenic soil carbonate is controlled by the type of plant cover (Cerling 1984).

The formation of authigenic soil carbonate has been described and its fractionation pathways under various types of plant cover have been documented by Cerling (1984), Quade *et al.* (1989) and Cerling *et al.* (1991). Since C4 plants were not a significant part of the flora until the Miocene (Quade & Cerling 1995) and the  $\delta^{13}\text{C}$  values of a C3 cover are between  $-14\text{‰}$  and  $-8\text{‰}$ , changes in the atmospheric  $^{13}\text{C}$ -to- $^{12}\text{C}$  ratio should be recorded in pedogenic carbonate (Cerling 1984; Quade *et al.* 1989; Cerling *et al.* 1991; Koch 1998). Evaporation

causes covariation in C and O in soil carbonate, both becoming enriched in the heavier isotope higher in the profile. Pedogenic carbonate forms in isotopic equilibrium with soil  $\text{CO}_2$ , which in turn is determined by the relative proportions of C3 and C4 plants where soil respiration rates are high enough to exclude isotopic inputs from atmospheric  $\text{CO}_2$  (Cerling 1984, 1991; Cerling & Hay 1986; Cerling *et al.* 1989; Quade *et al.* 1989; Cerling & Quade 1993). Terrestrial plants employ 3 distinct photosynthetic pathways reflecting different carbon isotopic fractionation. The bulk of continental plants (i.e. basically all trees, most shrubs and herbs, and cool-season and montane grasses) follow a C3 photosynthetic pathway (Calvin cycle). These display a range in  $\delta^{13}\text{C}$  values between  $-33\text{‰}$  and  $-21\text{‰}$  and average about  $-27\text{‰}$  (Cerling & Quade 1993). The C4 (Hatch-Slack) photosynthetic pathway is less discriminating against  $^{13}\text{C}$ , and therefore C4 plants (warm season grasses, sedges and a few halophytic shrubs) are higher in  $\delta^{13}\text{C}$  than C3 plants. They have  $\delta^{13}\text{C}$  values between  $-6\text{‰}$  and  $-19\text{‰}$  (Deines 1980) with an average of  $-13\text{‰}$ . The soil carbonates formed in the presence of pure C3 vegetation are between  $-14\text{‰}$  and  $-8\text{‰}$ , whereas

**Table 2.** Semiquantitative analysis of clay fraction of samples.

values above  $-8\text{‰}$  indicate a mixture of C3 and C4 plants (Cerling 1984; Cerling *et al.* 1991; Quade & Cerling 1995).

The stable isotope compositions of the Bala samples were measured relative to a standard, Vienna Standard Mean Ocean Water (VSMOW) or Vienna Pee Dee Belemnite (VPDB). They are expressed with delta notation ( $\delta$ ) in parts per thousand (‰ or per mil) (Table 4). The isotopic composition of carbonates in the Bala section exhibit a slightly wider range in  $\delta^{13}\text{C}$  composition from  $-5.98\text{‰}$  to  $-9.22\text{‰}$  and a narrower range in  $\delta^{18}\text{O}$  composition from  $-7.19\text{‰}$  to  $-8.66\text{‰}$ . The relative changes of the stable isotopes with respect to depth are plotted in Figure 6. The trends of stable isotopes start with a depletion at the bottom levels of B16, and then in the middle an enrichment is observed at B7. Next, a major depletion at B4 is recorded, finally ending with an enrichment at the top at the B2 level (Figure 6).

Comparing the  $\delta^{13}\text{C}$  values with  $\delta^{18}\text{O}$  values in the Bala section, almost parallel trends may be observed, except at the BC level where  $\delta^{13}\text{C}$  is higher with respect to the  $\delta^{18}\text{O}$  composition (Figure 6). A good covariance can be observed between the  $\delta^{13}\text{C}$  and  $\delta^{18}\text{O}$  values of carbonates in the Bala section. The ranges of stable isotope values are typical of a meteoric vadose environment (James & Choquette 1990). The high values of both  $\delta^{13}\text{C}$  and  $\delta^{18}\text{O}$  at the surficial horizons indicate the effect of water evaporation. When compared with the Sr composition of the same levels in the Bala section, increasing and decreasing trends in  $\delta^{13}\text{C}$  and  $\delta^{18}\text{O}$  diagrams correlate well with Sr enrichments and depletions, respectively. As might be expected to be

dominant in Mediterranean arid to semiarid climates, C3:C4 mixed flora is favoured in the palaeosols of the Bala section.

Fluid  $\delta^{18}\text{O}$  values are calculated using the calcite-water fractionation curve given by Friedman and O'Neil (1977) (Table 5). Assuming that the carbonates of the Bala section formed at  $0\text{ °C}$ , then the calculated  $\delta^{18}\text{O}$  values for the formation water range from  $-11\text{‰}$  to  $-13.1\text{‰}$ . If the soil temperatures vary between  $20\text{ °C}$  and  $30\text{ °C}$  and average  $25\text{ °C}$ , then the  $\delta^{18}\text{O}$  isotopic composition of the soil water in equilibrium with calcretes ranges from  $-4.9\text{‰}$  to  $-6.7\text{‰}$ . It has been observed for both temperature conditions that  $\delta^{18}\text{O}$  for waters has a range of roughly 2‰. Additionally,  $\delta^{18}\text{O}$  enrichment in the water equilibrated with calcretes is recorded in stratigraphic height, which means that the fluids were isotopically lighter at the beginning of calcrete formation and then became enriched with time as the maturity of the carbonates increased. During the early stages of carbonate accumulation within the Bala section, the soil water had a  $\delta^{18}\text{O}$  composition of less than  $-4.5\text{‰}$ . As Mack *et al.* (1991) stated, the waters with compositions exceeding  $-4\text{‰}$  imply high soil temperatures, in excess of  $30\text{ °C}$ . It was also mentioned in the same study that if the soil temperature were as cold as  $0\text{ °C}$ , the fluid  $\delta^{18}\text{O}$  values would become as light as  $-14\text{‰}$  to  $-12\text{‰}$ . If the formation temperature is assumed to be  $30\text{ °C}$ , then soil waters would have  $\delta^{18}\text{O}$  values ranging between  $-1\text{‰}$  and  $3\text{‰}$ . With the  $25\text{ °C}$  calculation,  $\delta^{18}\text{O}$  values of  $-4.9\text{‰}$  to  $-6.7\text{‰}$  were observed for Bala calcretes (Table 5). Therefore, neither temperatures of  $0\text{ °C}$  nor over  $25\text{ °C}$  are



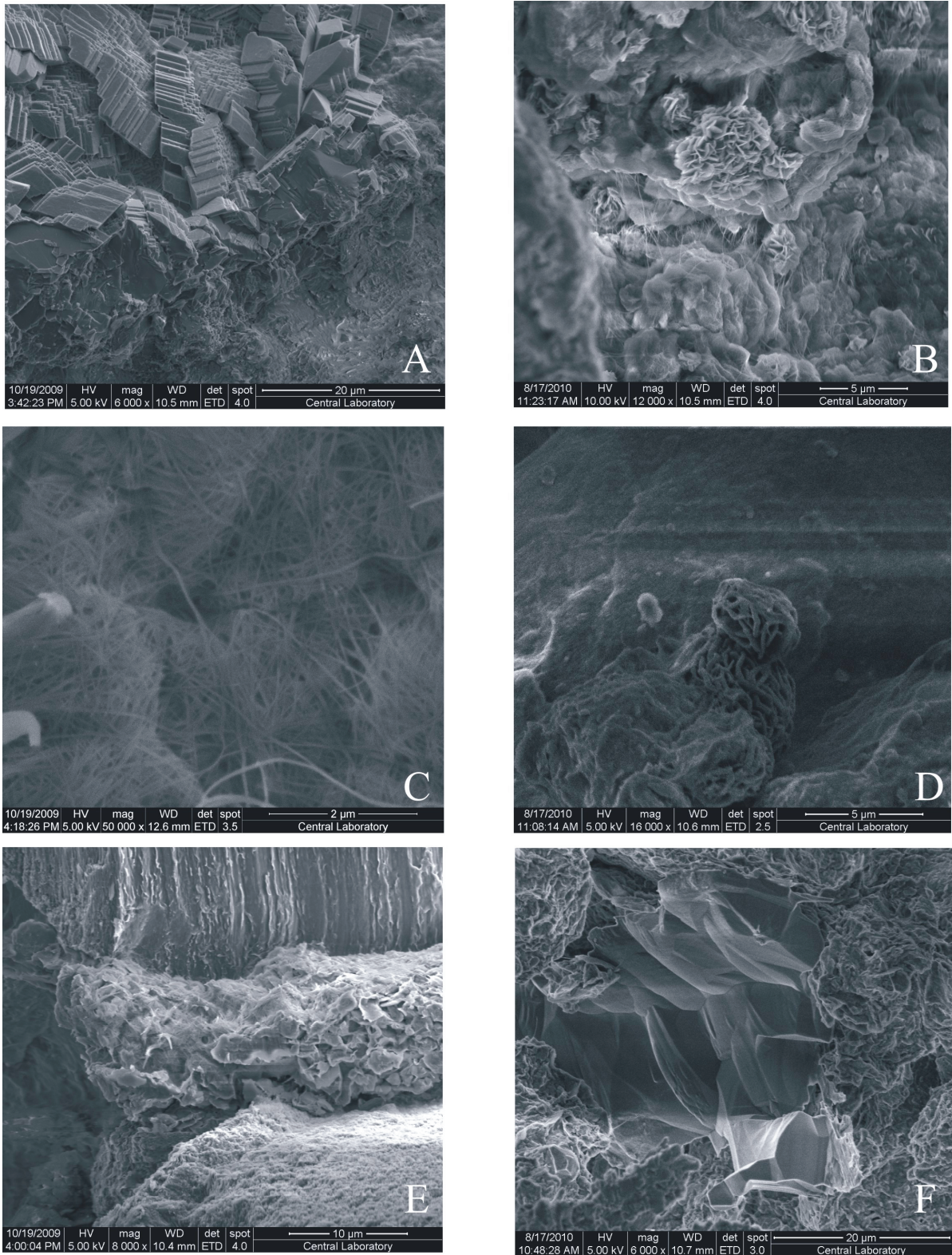


**Figure 5.** SEM images of: A) fresh surface of quartz grain showing conchoidal fracture; B) Palygorskite fibres forming bridge-like structure with authigenic formation of smectite nodules; C) Rhombohedral calcites coated with palygorskite fibres; D) Chlorite rosette; E) Subhedral feldspar grain, smectite and palygorskite formations; F) Rhombohedral calcite.

**Table 3.** Molecular weathering and pedogenesis ratios (from Retallack 2001 and Sheldon & Tabor 2009).

Ratio	Formula	Pedogenic Process
Al/ $\Sigma$ Bases	$Al_2O_3/(CaO+MgO+K_2O+Na_2O)$	Hydrolysis
Clayeyness	$Al_2O_3/SiO_2$	Hydrolysis
Base Loss	Ba/Sr	Leaching-Hydrolysis
Gleisation	$FeO/Fe_2O_3$	Oxidation
Gleisation	$\Sigma Fe/Al$	Oxidation
Gleisation	$\Sigma Fe+Mn/Al$	Oxidation
Silica/Sesquioxides	$SiO_2/(Fe_2O_3+Al_2O_3)$	Hydration
Base Loss	Base/Ti	Leaching
Provenance	Ti/Al	Acidification (~pH)
Alkalis to Alumina	$(K_2O+Na_2O)/Al_2O_3$	Salinisation
Soda to Potash	$Na_2O/K_2O$	Salinisation
Parent Material	La/Ce, Sm/Nd, U/Th	Acidification (~pH)

likely from the soil water temperatures for the carbonates of the Bala section. Based on the theoretical consideration, this study suggests that the surface water responsible for carbonate accumulation had  $\delta^{18}O$  values of probably less than  $-4\%$ , and possibly as low as  $-8\%$ , which assumes an approximately  $25\text{ }^\circ\text{C}$  soil depositional temperature.

### 5. Pleistocene climate archives from Ankara, Central Anatolia

The proxies in this study clearly show that semiarid and/or seasonally dry climatic conditions occurred in the region during the Quaternary. All of the data are compared in Figure 6. Dry periods, which are marked with grey areas, favour the formation of palygorskite and calcite while smectite decreases in amount (Figure 6). CIA-K values are low in dry periods while salinity and calcification are high, leading to high values of  $\delta^{13}C$  and  $\delta^{18}O$ . Towards the top of the section, the aridity is increasing, leading to the formation of calcretes, while in the lower levels, transient arid conditions do not show well-developed nodular calcretes but have powdery calcrete formations. The wet conditions, on the other hand, progress the pluvials and favour the formation of eluviation zones where leaching values are high. With age data on calcretes from the Bala section, the results can be compared with the global data.

The ages obtained in this section are highly significant, since the periodicity of glacial response changes from 41 ka to 100 ka in the Middle Pleistocene (Lisiecki & Raymo 2007), which was the beginning of the warmer periods lasting until the Holocene. Between 450 kyr and 780 kyr

ago, the interglacial periods favoured arid conditions over this region. Kapur *et al.* (1987) stated that the calcretes in southern Turkey were formed during the Middle Pleistocene interglacial periods. The calcretes dated in the Bala section are the lowest levels of the semimature nodular calcretes, where the lower ones are not calcretes but calcified soils. Therefore, the formation of calcretes in the Bala section at  $761 \pm 120$  ka coincides with the time of the climatic periodicity change. This time was also the time of the warming Mid-Brunhes Event (Kitaba *et al.* 2011).

### 6. A brief comparison of data with coeval archives from Turkey, the eastern Mediterranean and southern Europe

There are several published studies addressing the Quaternary palaeoclimates in Turkey, but most deal with the Holocene. The most recent work ( Eren *et al.* 2008; Eren 2011) described the stable isotopic compositions of Quaternary calcretes from Mersin in southern Turkey.  $^{18}O$  and  $^{13}C$  compositions of the Quaternary Mersin calcretes range from  $-4.31\%$  to  $-6.82\%$  and  $-6.03\%$  to  $-9.65\%$  PDB, respectively. These values are almost consistent with the stable isotope values of the studied calcretes. The calculated soil depositional temperature for the calcretes in the Mersin area ranges from  $25\text{ }^\circ\text{C}$  to  $32\text{ }^\circ\text{C}$ . It is also consistent with the soil depositional temperature of the studied calcretes, at approximately  $25\text{ }^\circ\text{C}$ . The strong covariance between the isotopic values of the Mersin calcretes was also recognised in the studied calcretes. This property was also identified in the carbonates of southern Europe (Sorbas Basin, Karlich Rhine Valley, Elsterian Loess,

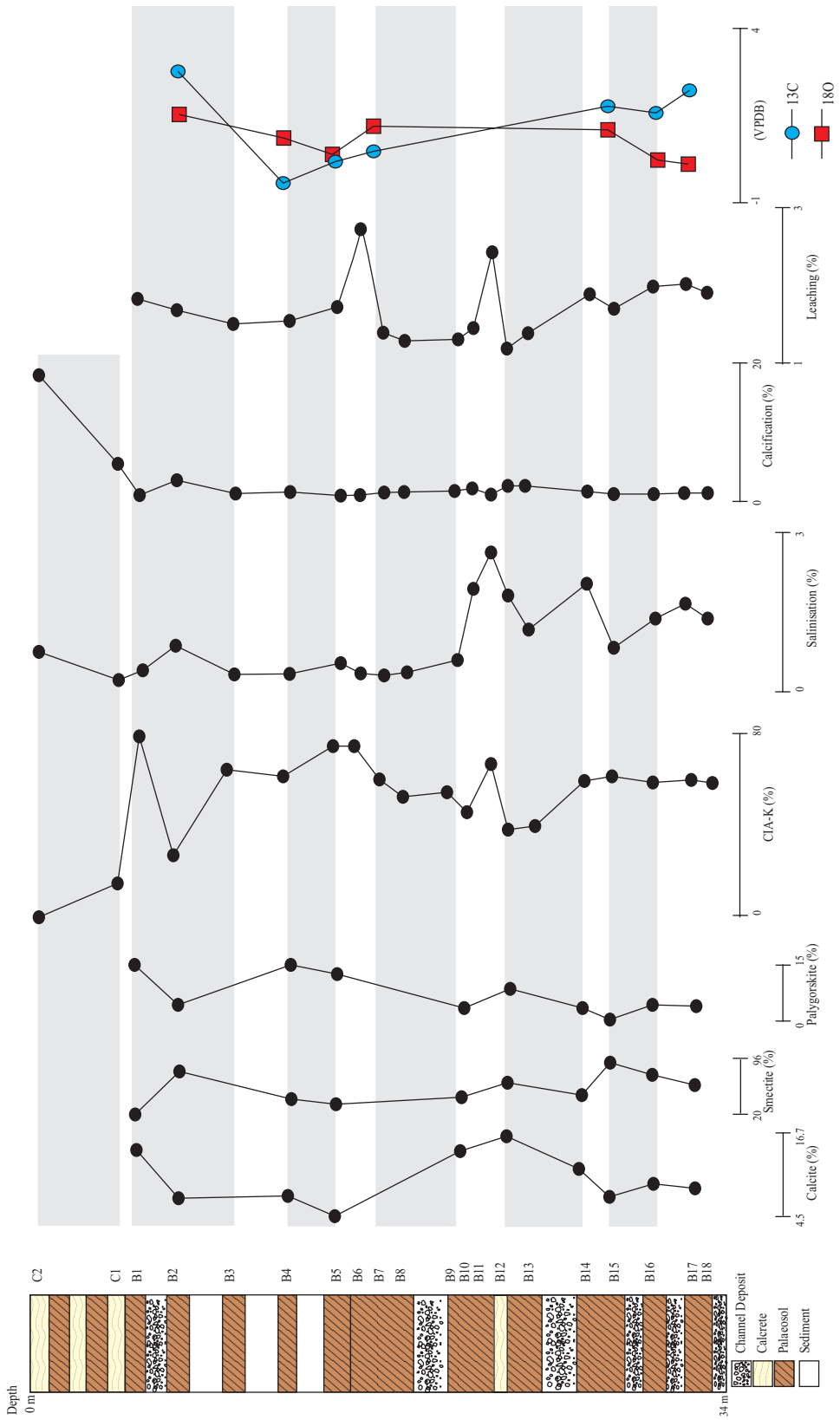


**Figure 6.** Interpretation of all proxy data of Bala section (grey areas show dry periods, the rest represents wet conditions).

**Table 4.**  $\delta^{13}\text{C}$  and  $\delta^{18}\text{O}$  isotope compositions of the samples.

Sample	$\delta^{13}\text{C}$	$\delta^{18}\text{O}$	$\delta^{18}\text{O}$
	VPDB	VSMOW	VPDB
B-2	-5.96	23.50	-7.19
B-4	-9.22	22.79	-7.88
B-5	-8.57	22.23	-8.42
BC	-8.32	23.11	-7.57
B-15	-6.99	23.02	-7.65
B-16	-7.15	22.08	-8.56
B-17	-6.50	21.98	-8.66

Holsteinian Palaeosol, Carbonates from Crete) (Candy *et al.* 2012). Like the isotopic covariance in southern Europe and the western and eastern Mediterranean carbonates, the studied calcretes have stable isotopic compositions, implying that their formation was controlled by the same environmental factors. However, the carbonates in western Europe, such as in England, for example, differ in that the isotopic values plot as scattered diagrams, indicating that their compositions have been controlled by different factors. Like in the study area, most of the carbonates in the Mediterranean region are soil carbonates. The stable isotope compositions of the studied carbonates are consistent with those of pedogenic soil carbonates from southern Europe and the Mediterranean. As Candy *et al.* (2012) suggested for the Mediterranean carbonates, aridity appears to be the major control on both  $\delta^{18}\text{O}$  and  $\delta^{13}\text{C}$  values in the studied soil carbonates with evaporation and  $\text{CO}_2$  degassing. This is confirmed by the low leaching

values during the dry seasons, favouring the formation of carbonate rich soil and/or calcretes.

### 7. Overall proxy evaluations and conclusions

This study reveals that there is consistency between the mineralogical compositions and molecular weathering ratios of the palaeosols and calcretes of the Bala section. The chemical index of alteration values show that the palaeosols were subjected to medium and high degrees of weathering, whereas low values were determined for the calcretes. Calcretes are pedogenic in origin, but semimature calcretes formed in the vadose zone of the depositional environment. The studied calcretes are powdery to nodular in form, whereas the palaeosols show prismatic to subangular-angular blocky and granular structures developed with horizons.

Palygorskite in the calcrete section is most probably pedogenic, where the Mg needed for palygorskite was

**Table 5.** The calculated  $\delta^{18}\text{O}$  values of the fluids responsible for the formation of the carbonates in Bala palaeosols.

Sample	Bala Section			Calculated Fluid $\delta^{18}\text{O}$ (SMOW)	
	$\delta^{13}\text{C}$	$\delta^{18}\text{O}$	$\delta^{18}\text{O}$	0 °C	25 °C
	VPDB	VSMOW	VPDB	VSMOW	VSMOW
B-2	-5.96	23.5	-7.19	-11	-4.9
B-4	-9.22	22.79	-7.88	-11.8	-5.8
B-5	-8.57	22.23	-8.42	-12.4	-6.4
BC	-8.32	23.11	-7.57	-11.6	-5.5
B-15	-6.99	23.02	-7.65	-11.5	-5.6
B-16	-7.15	22.08	-8.56	-13	-6.6
B-17	-6.5	21.98	-8.66	-13.1	-6.7

provided from smectite through the soil solution. The increase in palygorskite with calcite in the Bala section with decreasing smectite contents manifests the increasing aridity and the prevalence of the dry season. Chlorite, kaolinite and illite are the detrital clay minerals found in the studied samples.

The reddish soils reveal that the main soil-forming process in the region was calcification, whereas the brown soils reveal a less vigorous leaching/reddening and calcification-decalcification trend. The evolution history of the calcretes in the Çukurova Basin proposed by Kapur *et al.* (1990) is also valid for the calcretes in the Ankara region.

The stable isotope values of the studied samples are consistent with each other, indicating formation from percolating soil solutions under predominantly C4 to C3:C4 association-type vegetation. Temperature calculations show that the palaeoclimatic conditions favouring the formation of calcretes in the region are semiarid and seasonally dry with pluvial alternations. The estimated maximum soil depositional temperature for the formation of calcretes is calculated as approximately 25 °C.

ESR ages of the 2 calcrete levels fall within the Middle Pleistocene, when the MBE occurred and the climatic periodicity changed, affecting the climatic control over the European continent. This period is the time dated on

the Bala calcretes, documenting that the calcretes in the study area started to develop with the MBE, which led to high temperatures and probably the formation of almost all Mediterranean-type calcretes.

The studied calcretes present many similarities in mineralogical and isotope compositions with the calcretes in Mersin, southern Turkey. The latter are also Mid-Late Pleistocene in age. The stable isotope values of the studied calcretes in Bala are consistent with those of the Mersin calcretes from Turkey and many other coeval calcretes from southern Europe and the Mediterranean. This study suggests that smectite and palygorskite contents of the soils with the carbon and oxygen isotope compositions of the carbonates/carbonate-rich soils indicate aridity and/or seasonally dry conditions in the Mediterranean during the Middle Pleistocene, triggering the formation of soil carbonates and/or calcretes.

### Acknowledgements

This study is a part of a PhD thesis completed by the first author, which was financially supported by TÜBİTAK under project 106Y172. The authors are grateful to Prof Dr Fred J Longstaffe from the University of Western Ontario, Canada, for his help during stable isotope analysis of the samples. The reviewers of this manuscript are thanked for their constructive comments.

### References

- Akçay, A.E., Dönmez, M., Kara, H., Yergök, A.F. & Esentürk, K. 2008. 1:100 000 Ölçekli Türkiye Jeoloji Haritaları Kırşehir J-30 Paftası [Geological Maps of Turkey in 1:100,000 Scale, Kırşehir J-30 Sheet]. MTA Publications No: 91, Ankara.
- Akyürek, B., Duru, M., Sütçü, Y.F., Papak, D., Aroğlu, F., Pehlivan, N., Gönenç, O., Granit, S. & Yaar, T. 1997. 1:100 000 Ölçekli Türkiye Jeoloji Haritaları Ankara F-15 Paftası [Geological Maps of Turkey in 1:100,000 Scale, Ankara F-15 Sheet]. MTA Publications No: 55, Ankara.
- Biscaye, P.E. 1965. Mineralogy and sedimentation of recent deep sea clay in the Atlantic Ocean and adjacent seas and oceans. *Geological Society of America Bulletin* **76**, 803–832.
- Bottema, S., Woldring, H. & Aytuğ, B. 1993/1994. Late Quaternary vegetation history of northern Turkey. *Palaeohistoria* **35/36**, 13–72.
- Bradley, R.S. 1999. *Paleoclimatology: Reconstructing Climates of the Quaternary*. Academic Press, San Diego.
- Brindley, G.W. 1980. Quantitative X-ray analyses of clays. In: Brindley, G.W. & Brown, G. (eds), *Crystal Structures of Clay Minerals and their X-ray Identification*. Mineralogical Society Monograph **5**, 411–438.
- Buol, S.W., Hole, F.D., McCracken, R.J. & Southard, R.J. 1997. *Soil Genesis and Classification*. Iowa State University Press, Ames, Iowa.
- Candy, I., Adamson, K., Gallant, C.E., Whitfield, E. & Rope, R. 2012. Oxygen and carbon isotopic composition of Quaternary meteoric carbonates from western and southern Europe: their role in palaeoenvironmental reconstruction. *Palaeogeography, Palaeoclimatology, Palaeoecology* **326–328**, 1–11.
- Candy, I., Coope, G.R., Lee, J.R., Parfitt, S.A., Preece, R.C., Rose, J. & Schreve, D.C. 2010. Pronounced warmth during early Middle Pleistocene interglacials: investigating the Mid-Brunhes Event in the British terrestrial sequence. *Earth-Science Reviews* **103**, 183–196.
- Cangir, C. & Kapur, S. 1984. Ankara-Dikmen Paleosol Toprağının Çevresindeki Pedolitler ile Toposequens İlişkisi ve Ankara Kilinin Minerolojik özellikleri [Toposequential Relationship between Pedoliths of Ankara-Dikmen Palaeosols and Ankara Clay]. I. Ulusal Kil Sempozyumu Bildirileri, Adana, 261–279.
- Cerling, T.E. 1984. The stable isotopic composition of modern soil carbonate and its relationship to climate. *Earth and Planetary Science Letters* **71**, 229–240.
- Cerling, T.E. 1991. Carbon dioxide in the atmosphere: evidence from Cenozoic and Mesozoic paleosols. *American Journal of Science* **291**, 377–400.
- Cerling, T.E. & Hay, H.L. 1986. An isotopic study of paleosol carbonates from Olduvai Gorge. *Quaternary Research* **25**, 63–78.

- Cerling, T.E. & Quade, J. 1993. Stable carbon and oxygen isotopes in soil carbonates. In: Swart, P.K., Lohmann, K.C., McKenzie, J. & Savin S. (eds), *Climate Change in Continental Isotopic Records*. Geophysical Monographs **78**, 217–231.
- Cerling, T.E., Solomon, D.K., Quade, J. & Bowman, J.R. 1991. On the isotopic composition of carbon in soil carbon dioxide. *Geochimica et Cosmochimica Acta* **55**, 3403–3405.
- Deines, P. 1980. The isotopic composition of reduced organic carbon. In: Fritz, P. & Fontes, J.Ch. (eds), *Handbook of Environmental Isotope Geochemistry*, Vol. 1. Elsevier, New York, 329–406.
- Dönmez, M., Akçay, A.E., Kara, H., Yergök, A.F. & Esebürk, K. 2008. 1:100 000 Ölçekli Türkiye Jeoloji Haritaları Kırşehir I-30 Paftası [Geological Maps of Turkey in 1:100,000 Scale, Kırşehir I-30 Sheet]. MTA Publications No: 91, Ankara.
- Eastwood, W.J., Roberts, N., Lamb, H.F. & Tibby, J.C. 1999. Holocene environmental change in southwest Turkey. A palaeoecological record of lake and catchment-related changes. *Quaternary Science Reviews* **18**, 671–696.
- Eren, M. 2011. Stable isotope geochemistry of Quaternary calcretes in the Mersin area, southern Turkey – A comparison and implications for their origin. *Chemie der Erde* **71**, 31–37.
- Ermolli, E.R. & Cheddadi, R. 1997. Climatic reconstruction during the Middle Pleistocene: a pollen record from Vallo di Diano (Southern Italy). *Geobios* **30**, 735–744.
- Erol, O. 1956. Ankara güneydoğusundaki Elma Dağı ve çevresinin jeolojisi ve jeomorfolojisi üzerine bir araştırma [A research on the geology and geomorphology of Elma Mountain (southeast of Ankara) and its vicinity]. MTA Publications D.9, Ankara.
- Erol, O. 1961. Ankara Bölgesinin Tektonik Gelişmesi [Tectonic Development of Ankara Region]. *TJK Bulletin*, 57–85.
- Erol, O. 1973. Ankara şehri çevresinin jeomorfolojik ana birimleri [Major geomorphological units of Ankara Region]. Ankara University Faculty of Languages, History and Geography Publications **240**, 29.
- Erol, O. 1983. Türkiye'nin genç tektonik ve jeomorfolojik gelişimi [Recent tectonism and geomorphology of Turkey]. *Jeomorfoloji* **11**, 1–22.
- Fontugne, M., Kuzucuoğlu, C., Karabıykoğlu, M., Hatte, C. & Pestre, J.F. 1999. From Pleniglacial to Holocene: a <sup>14</sup>C chronostratigraphy of environmental changes in the Konya Plain, Turkey. *Quaternary Science Reviews* **18**, 573–591.
- Friedman, I. & O'Neil, J.R. 1977. Compilation of stable isotope fractionation factors of geochemical interest. In: Fleischer, M. (ed), *Data of Geochemistry*. USGS Prof. Paper 440-KK, 1–12.
- Göktürk, O.M., Fleitmann, D., Badertscher, S., Cheng, H., Edwards, R.L., Leuenberger M., Fankhauser, A., Tüysüz, O. & Kramers, J. 2011. Climate on the southern Black Sea coast during the Holocene: implications from the Sofular Cave record. *Quaternary Science Reviews* **30**, 2433–2445.
- Goudie, A.S. 1973. *Duricrusts in Tropical Landscapes*. Clarendon Press, Oxford.
- Goudie, A.S. 1983. Calcrete. In: Goudie, A.S. & Pye, K. (eds), *Chemical Sediments and Geomorphology*. Academic Press, London, 93–131.
- Gündoğdu, M.N. 1982. *Geological, Mineralogical and Geochemical Investigation of the Bigadiç Neogene Volcano-Sedimentary Basin*. PhD Thesis, Hacettepe University, Ankara, Turkey [unpublished].
- Imbrie, J., Berger, A., Boyle, E.A., Clemens, S.C., Duffy, A., Howard, W.R., Kukla, G., Kutzbach, J., Martinson, D.G., McIntyre, A., Mix, A.C., Molino, B., Morley, J.J., Peterson, L.C., Pisias, N.G., Prell, W.L., Raymo, M.E., Shackleton, N.J. & Toggweiler, J.R. 1993. On the structure and origin of major glacial cycles. 2 The 100,000 year cycle. *Paleoceanography* **8**, 699–735.
- Jackson, M.L. 1979. Soil chemical analysis - advanced course, 2nd edition. Published by the author, Madison, Wisconsin.
- James, N.P. 1972. Holocene and Pleistocene calcareous crust (caliche) profiles: Criteria for subaerial exposure. *Journal of Sedimentary Petrology* **42**, 817–836.
- James, N.P. & Choquette, P.W. 1990. Limestones – the sea floor diagenetic environment. In: McIlreath, A & Morrow, D.W. (eds), *Diagenesis*. Geosci. Canada Report Ser. **4**, 13–34.
- Kapur, S., Çavuşgil, V.S. & Fitzpatrick, E.A. 1987. Soil–calcrete (caliche) relationship on a Quaternary surface of the Çukurova Region, Adana (Turkey). In: Federoff, N., Bresson, L.M., & Courty, M.A. (eds), *Soil Micromorphology*. Association Francaise pour L'Etude du sol, Paris, 597–603.
- Kapur, S., Saydam, C., Akça, E., Çavuşgil, V.S., Karaman, C., Atalay, I. & Özsoy, T. 2000. Carbonate pools in soil of the Mediterranean: a case study from Anatolia. In: Lal, R., Kimble, J.M., Eswaran, H. & Stewart, B.A. (eds), *Global Climate Change and Pedogenic Carbonates*. Lewis Publishers, Boca Raton, Florida, 187–212.
- Kitaba, I., Harada, M., Hyodo, M., Katoh, S., Sato, H. & Matsushita, M. 2011. MIS 21 and the Mid-Pleistocene climate transition: climate and sea-level variation from a sediment core in Osaka Bay, Japan. *Palaeogeography, Palaeoclimatology, Palaeoecology* **299**, 227–239.
- Koch, P.L. 1998. Isotopic reconstruction of past continental environments. *Annual Review of Earth and Planetary Sciences* **26**, 573–613.
- Koçyiğit, A. 1987. Hasanoğlan (Ankara) Yöresinin Tektono-Stratigrafisi: Karakaya Orojenik Kuşağının Evrimi [Tectono-stratigraphy of Hasanoğlan (Ankara): Evolution of Karakaya Orogenic Belt]. *Yerbilimleri* **14**, 269–293.
- Koçyiğit, A. 1991. An example of an accretionary forearc basin from northern Central Anatolia and its implications for the history of subduction of Neo-Tethys in Turkey. *Geological Society of America Bulletin* **103**, 22–36.
- Koçyiğit, A. 2000. General neotectonic characteristics and seismicity of Central Anatolia. Haymana-Tuzgözü-Ulukıla Basenleri Uygulamalı Çalışma. *Türkiye Petrol Jeologları Derneği Özel Sayı* **5**, 1–26.
- Küçükuysal, C. 2011. Palaeoclimatological Approach to Plio-Quaternary Paleosol-Calcrete Sequences in Bala and Gölbaşı (Ankara) by Using Mineralogical and Geochemical Proxies. PhD Thesis, Middle East Technical University, Ankara, Turkey.
- Küçükuysal, C., Engin, B., Türkmenoğlu, A.G. & Aydaş, C. 2011. ESR dating of calcrete nodules from Bala, Ankara (Turkey): preliminary results. *Applied Radiation and Isotopes* **69**, 492–499.

- Kuzucuoglu, K.C., Bertaux, J., Black, S., Deneffe, M., Fontugne, M., Karabiyikoglu, M., Kashima, K., Limondin-Lozouet, N., Mouralis, D. & Orth, P. 1999. Reconstruction of climate changes during the upper Pleistocene, based on sediment records from the Konya Basin (Central Anatolia, Turkey). *Geological Journal* **34**, 175–198.
- Lisiecki, L.E. & Raymo, M.E. 2007. Plio-Pleistocene climate evolution: trends and transitions in glacial cycle dynamics. *Quaternary Science Reviews* **26**, 56–69.
- Litt, T., Krastel, S., Sturm, M., Kipfer, R., Örcen, S., Heumann, G., Franz, S.O., Ülgen, U.B. & Niessen, F. 2009. 'PALEOVAN', International Continental Scientific Drilling Program (ICDP): site survey results and perspectives. *Quaternary Science Reviews* **28**, 1555–1567.
- Mack, G.H., Cole, D.R., Giordano, T.H., Schaal, W.C. & Barcelos, J.H. 1991. Paleoclimatic controls on stable oxygen and carbon isotopes in caliche of the Abo Formation (Permian), south-central New Mexico, U.S.A. *Journal of Sedimentary Petrology* **61**, 458–472.
- Moore, D.M. & Reynolds, J.R. 1989. *X-ray Diffraction and the Identification and Analysis of Clay Minerals*. Oxford University Press, Oxford.
- Nesbitt, H.W. & Young, G.M. 1982. Early Proterozoic climates and plate motions inferred from major element chemistry of lutites. *Nature* **299**, 715–717.
- Quade, J. & Cerling, T.E. 1995. Expansion of C4 grasses in the late Miocene of northern Pakistan: evidence from stable isotopes in paleosols. *Palaeogeography, Palaeoclimatology, Palaeoecology* **115**, 91–116.
- Quade, J., Cerling, T.E. & Bowman, J.R. 1989. Systematic variations in the carbon and oxygen isotopic composition of pedogenic carbonate along elevation transects in the southern Great Basin, United States. *Geological Society of America Bulletin* **101**, 464–475.
- Pisias, N.G. & Moore, T.C. 1981. The evolution of the Pleistocene climate: a time series approach. *Earth and Planetary Science Letters* **52**, 450–458.
- Retallack, G.J. 1997. *A Colour Guide to Paleosols*. Wiley, Chichester.
- Retallack, G.J. 2001. *Soils of the Past*. Blackwell, Oxford.
- Roberts, N., Reed, J., Leng, M.J., Kuzucuoglu, C., Fontugne, M., Bertaux, J., Woldring, H., Bottema, S., Black, S., Hunt, E. & Karabiyikoglu, M. 2011: The tempo of Holocene climatic change in the eastern Mediterranean region: new high-resolution crater-lake sediment data from central Turkey. *The Holocene* **11**, 721–36.
- Ruddiman, W.F., Raymo, M.E., Martinson, D.G., Clement, B.M. & Backman, J. 1989. Pleistocene evolution: northern hemisphere ice sheets and North Atlantic Ocean. *Paleoceanography* **4**, 353–412.
- Salomons, W., Goudie, A. & Mook, W.G. 1978. Isotopic composition of calcrete deposits from Europe, Africa and India. *Earth Surface Processes* **3**, 43–57.
- Sheldon, N.D. & Tabor, N.J. 2009. Quantitative paleoenvironmental and paleoclimatic reconstruction using paleosols. *Earth-Science Reviews* **95**, 1–52.
- Tabor, N.J. 2002. *Paleoclimate Isotopic Proxies Derived from Paleozoic, Mesozoic, Cenozoic Paleosols and Modern Soils*. PhD thesis, University of California, Davis, California.
- Thorez, J. 1976. *Practical Identification of Clay Minerals*. Lelotte, Dison, Belgium.
- Tucker, M.E. 1991. *Sedimentary Petrology: An Introduction to the Origin of Sedimentary Rocks*. Blackwell Science, Oxford.
- Wick, L., Lemcke, G. & Sturm, M. 2003. Evidence of Lateglacial and Holocene climatic change and human impact in eastern Anatolia: high resolution pollen, charcoal, isotopic and geochemical records from the laminated sediments of Lake Van, Turkey. *The Holocene* **13**, 665–675.
- Wright, V.P. & Tucker, M.E. 1991. *Calcretes*. Blackwell Science, Oxford.